In-plane crashworthiness of bio-inspired hierarchical honeycombs

Hanfeng Yin [a], Xiaofei Huang [a], Fabrizio Scarpa [b], Guilin Wen [a], Yanyu Chen [c*], and Chao Zhang [d]

[a] State Key Laboratory of Advanced Design and Manufacturing for Vehicle Body, Hunan University, Changsha, Hunan 410082, PR China

[b] Bristol Composites Institute (ACCIS), University of Bristol, Bristol, BS8 1TR, UK

[c] Transportation and Hydrogen Systems Center, National Renewable Energy Laboratory, 15013 Denver West Parkway, Golden CO 80401, USA

[d] School of Aeronautics, Northwestern Polytechnical University, Xi'an, Shanxi 710072, PR China

* Corresponding author: Y. Chen, E-mail: yanyu.chen@nrel.gov, Tel: +1-303-275-4445

Abstract: Biological tissues like bone, wood, and sponge possess hierarchical cellular topologies, which are lightweight and feature an excellent energy absorption capability. Here we present a system of bio-inspired hierarchical honeycomb structures based on hexagonal, Kagome, and triangular tessellations. The hierarchical designs and a reference regular honeycomb configuration are subjected to simulated in-plane impact using the nonlinear finite element code LS-DYNA. The numerical simulation results show that the triangular hierarchical honeycomb provides the best performance compared to the other two hierarchical honeycombs, and features more than twice the energy absorbed by the regular honeycomb under similar loading conditions. We also propose a parametric study correlating the microstructure parameters (hierarchical length ratio r and the number of sub cells N) to the energy absorption capacity of these hierarchical honeycombs. The triangular hierarchical honeycomb with $N = 2$ and $r = 1/8$ shows the highest energy absorption capacity among all the investigated cases, and this configuration could be employed as a benchmark for the design of future safety protective systems.

Keywords: hierarchical structure, honeycomb, impact, energy absorption, crashworthiness

1. Introduction

Honeycomb structures have been widely used in aerospace engineering, mechanical, and civil engineering due to their excellent mechanical performance and lightweight characteristic [1]. The hexagonal honeycomb is a suitable material for protective and packaging applications because of its excellent energy absorption capacity [2, 3]. In the past decades, a significant number of researchers have investigated the crashworthiness of honeycomb structures using theoretical, experimental, and numerical simulation methods. Wierzbicki [4] made use of the super folding element theory to analysis the crashworthiness of the hexagonal honeycomb structure under the out-of-plane loading. The theoretical prediction showed that the crashworthiness of a honeycomb bears strict relations with the core material, the wall thickness, and width. Wu and Jiang [5] have carried out experimental studies on six types of aluminum honeycombs under quasi-static and dynamic out-of-plane loading. The experimental results showed that the dynamic crushing strength was significantly higher than the quasi-static crushing strength. Cricrì *et al*. [6], Papka and Kyriakides [7], and Ruan *et al*. [8] investigated the behavior of regular hexagonal honeycombs under in-plane loading using numerical simulations. The results show that the numerical methods can provide high fidelity predictions of the deformation modes and the crushing forces of the honeycomb topology.

The investigations above have focused on honeycombs with one-order cellular configurations. Natural materials like wood, bone, and sponge have, however, hierarchical cellular structures, i.e., higher-order ones [9, 10]. Arguably the hierarchical configuration explains why these classes of natural materials possess good energy absorption, as well as high lightweight characteristic. For this reason, several research groups have investigated the mechanical performance of hierarchical structures. Chen *el al.* [11] reported a class of hierarchically architected honeycombs with simultaneous prominent wave attenuation and load-carrying capabilities. The mechanisms responsible for the broad phononic band gaps and enhanced stiffness depend on the geometric features of the hierarchical honeycombs rather than their composition. Zheng *et al*. [12] have fabricated a novel metallic hierarchical metamaterial with several three-dimensional features spanning up to seven orders of magnitude, from nanometers to centimeters. This novel metallic hierarchical metamaterial was found to have a significantly higher specific strength compared to aluminum, stainless

steel, and titanium foams, as well as silica aerogel and Al_2O_3 nanolattices. Vigliotti and Pasini [13] have evaluated the improvement in terms of stiffness and strength of lattices with multiple hierarchical levels compared to traditional structures. Sun *et al*. [14] have designed a hierarchical triangular lattice with lattice-core sandwich walls. The axial crushing experimental results of the hierarchical topology show a significantly higher crashworthiness than the single-cell and the multi-cell lattice structure. Additionally, Zheng *et al*. [15] have investigated the behavior of hierarchical woven lattice composites and found that hierarchical lattice structures provide a significant boost to the energy absorption capability of the lightweight woven textile material compared with the non- hierarchical configuration.

Hierarchical hexagonal honeycombs, which combine the advantages of the regular hexagonal configuration in order one and possess a nested hierarchical structure, are extremely promising for crashworthiness applications. Zhang *et al*. [16] and Sun *et al*. [17] have investigated the axial crushing behaviors in self-similar regular hierarchical honeycombs using an explicit finite element code. The results show that the first-order and the second-order hierarchical honeycomb improve the specific energy absorption by 81% and 186% compared to the regular hexagonal honeycomb, respectively. Zhao *et al*. [18] designed and tested configurations of hierarchical composite honeycombs (HCHs). HCHs were found to possess remarkable specific energy absorption. Sun *et al*. [19, 20] have evaluated the in-plane stiffness of these hierarchical honeycombs, which was significantly higher than that of the regular honeycomb. Chen and Pugno [21, 22] have analyzed the in-plane elastic buckling properties of hierarchical honeycombs and the in-plane elastic properties of hierarchical nano-honeycombs. Qiao *et al*. [23] have in particular investigated the crashworthiness performance of a second order hierarchical honeycomb under in-plane loading by using theoretical analyses and finite element simulations. The results gathered from these two modeling techniques have clearly shown that the hierarchical honeycomb concept provides an improved energy absorption capacity over traditional hexagonal and triangular honeycombs. More recently, Chen *et al*. [24] have fabricated one type of hierarchical honeycombs using commercial 3D printers. Their experimental results indicate that the 3D printed hierarchical honeycombs exhibit a progressive failure mode under uniaxial compression along with improved stiffness and energy absorption. Remarkably, these

hierarchical honeycombs also exhibit high energy dissipation at large imposed strains (up to 60%) under cyclic loading.

The aforementioned studies on the mechanical performance of hierarchical honeycombs are, however, focused on the regular honeycomb configuration, with cell walls consisting of only one topological type of substructure. Here we propose three different types of hierarchical honeycombs with various topological substructures (i.e., the hexagonal, Kagome and triangular honeycombs), all subjected to in-plane dynamic loading conditions and their in-plane energy absorption capacity explored. The paper is organized as follows. The structural description of the proposed hierarchical honeycombs and the finite element modeling are presented in Section 2. The dynamic in-plane properties of the honeycombs are studied and discussed in Section 3. The main conclusions are summarized in Section 4.

2. Hierarchical honeycombs and their finite element models

2.1. Structural description

The cross-section configurations of the three hierarchical honeycombs and the regular honeycomb evaluated in this work are presented in **Fig. 1** (a) and (b). The three types of hierarchical honeycombs are constructed by substituting the cell walls of the regular honeycomb with the corresponding cellular structure (i.e., hexagonal, Kagome and triangular honeycombs). The detailed configurations of these cellular structures are shown in **Fig. 1** (c).

We introduce two geometric parameters to describe the topology of the proposed hierarchical honeycombs. The first design parameter is the hierarchical length ratio $r = l_h / l_0$, where l_h is the cell wall length of the hexagonal hierarchical honeycomb, and l_0 denotes the length of the cell wall of the regular (level 0) honeycomb. The other design parameter used in this work is N, which represents the number of complete sub cells away from the central axis of each cell wall. As an example, **Fig. 2** shows the configurations of three different hierarchical honeycombs with $N = 1$, 2 and 3 and $r = 1/8$.

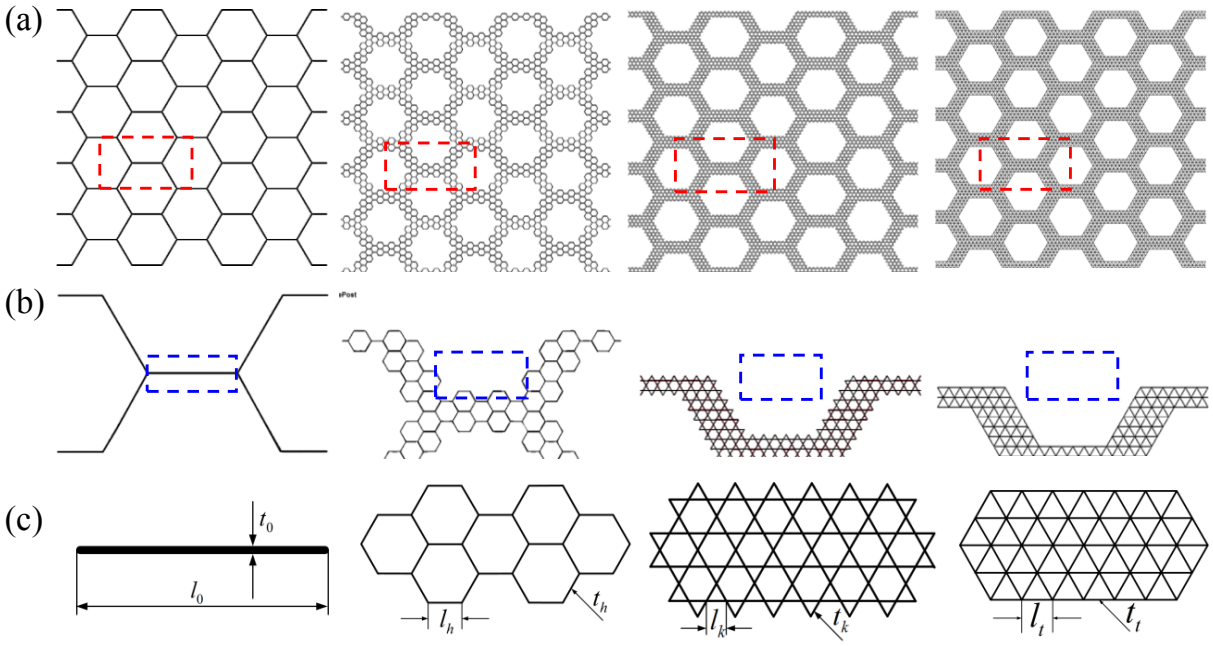

Fig. 1. Geometrical illustrations of the proposed hierarchical honeycombs. (a) Regular honeycomb, hexagonal hierarchical honeycomb, Kagome hierarchical honeycomb, and triangular hierarchical honeycomb. (b) Representative volume element of each type of honeycomb. (c) The corresponding cell wall of each type of honeycomb. Here $r = 1/8$ and $N = 1$.

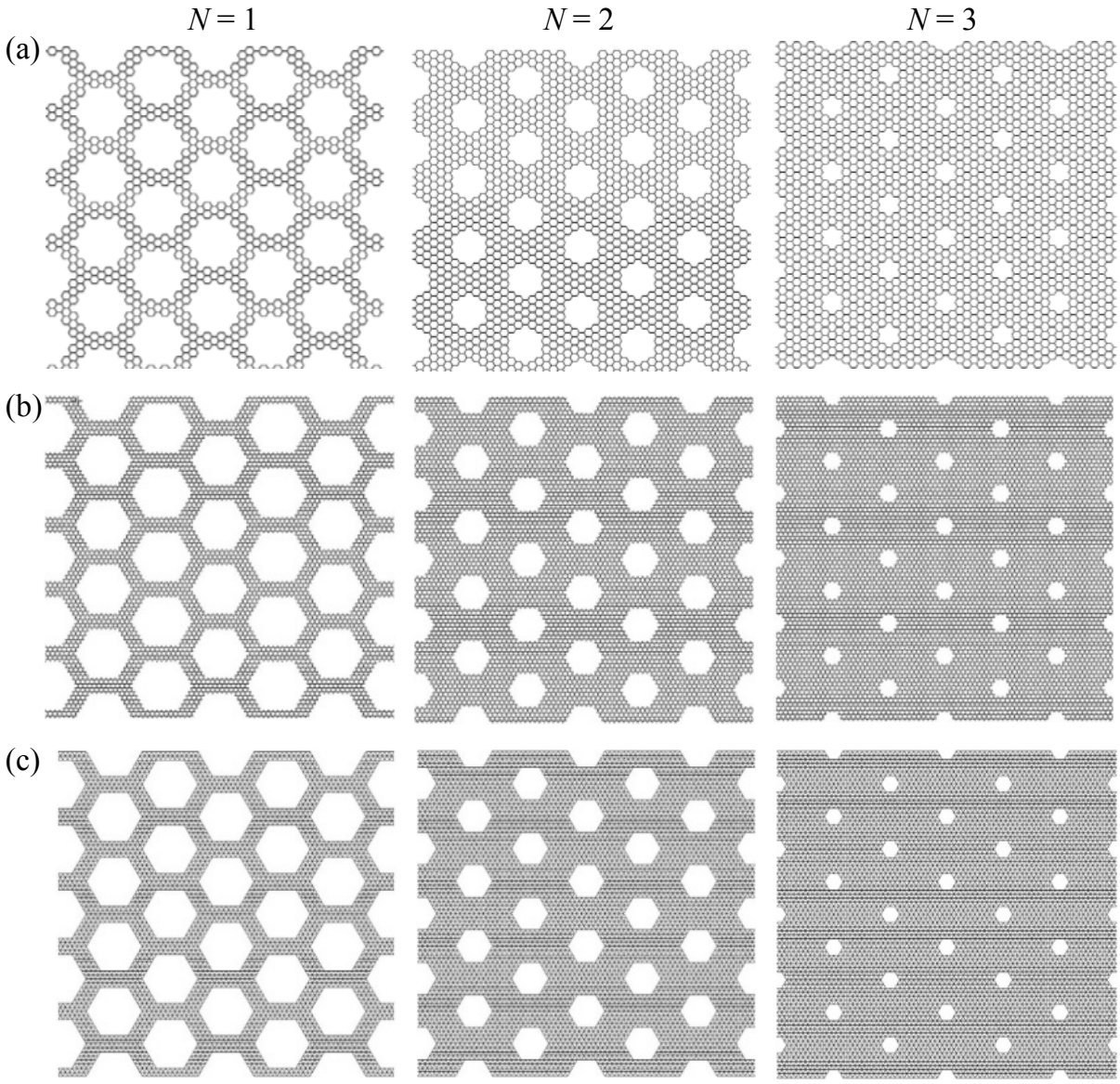

Fig. 2. The configurations of hierarchical honeycombs with N = 1, 2 and 3. (a) Hexagonal, (b) Kagome and (c) triangular. Here r = 1/8.

For the purpose of comparison, all results have been acquired for configurations having equivalent mass by imposing the following condition [25]:

$$t_0 l_0 - \frac{t_0^{\,2}}{2\sqrt{3}} = 3P\left(t_h l_h - \frac{t_h^{\,2}}{2\sqrt{3}} \right) \tag{1}$$

In Eq. (1), t_0 and l_0 represent the thickness and the length of the cell of a regular honeycomb (always at level 0). The simulations carried out in this work have been performed by fixing l_0 = 20 mm, t_0=0.8 mm, and an out-of-plane thickness of 10 mm. As a result, the relative density for all of the considered honeycombs is 0.05. The parameters t_h and l_h in Eq. (1) are the

thickness and length of the cell wall of the nested hexagonal lattice, respectively. P indicates the number of hexagonal nested cells with one-half thickness and is determined by N and r.

From Eq. (1), one can extract the thickness and the length of the hexagonal hierarchical lattice as:

$$\frac{t_h}{l_h}=\frac{\sqrt{3}}{2}\left\{1-\sqrt{1-\frac{16}{Q\gamma^2 3\sqrt{3}}\left[\frac{t_0}{l_0}-\frac{1}{2\sqrt{3}}\left(\frac{t_0}{l_0}\right)^2\right]}\right\} \tag{2}$$

Similarly, the thickness and the length of the Kagome and triangular hierarchical honeycombs can be calculated as:

$$\frac{t_k}{l_k}=\frac{\sqrt{3}}{2}\left\{1-\sqrt{1-\frac{16}{Q\gamma^2 3\sqrt{3}}\left[\frac{t_0}{l_0}-\frac{1}{2\sqrt{3}}\left(\frac{t_0}{l_0}\right)^2\right]}\right\} \tag{3}$$

$$\frac{t_t}{l_t}=\frac{1}{\sqrt{3}}\left\{1-\sqrt{1-\frac{4\sqrt{3}}{3R\gamma^2}\left[\frac{t_0}{l_0}-\frac{1}{2\sqrt{3}}\left(\frac{t_0}{l_0}\right)^2\right]}\right\} \tag{4}$$

In Eq. (3) and Eq. (4), t_k and l_k are the thickness and length of the Kagome lattices; t_t and l_t otherwise represent the thickness and the length of the triangular lattice. The number of hierarchical cells for the Kagome and triangular lattices are Q and R, respectively.

The test configurations considered in this work are shown in Table 1. Some particular topologies were not evaluated, for example, Kagome and triangular hierarchical honeycombs with at N = 3, and other configurations for r = 1/14. For r = 1/5, the maximum value of N considered in this work is 2. In the other cases, the size of the finite element models is extremely large and would have required massive computational efforts beyond our current capabilities.

Table1. Illustrations of the investigation cases.

	N	*r*			
Hexagonal	1	1/5	1/8	1/11	1/14
	2	1/5	1/8	1/11	/
	3	/	1/8	1/11	/
Kagome	1	1/5	1/8	1/11	/
	2	1/5	1/8	1/11	/
	3	/	1/8	1/11	/

	1	1/5	1/8	1/11	1/14
Triangular	2	1/5	1/8	1/11	/
	3	/	1/8	1/11	/

2.2. Finite element modeling

The finite element model consists of three parts: two rigid plates and the hierarchical honeycomb confined within those plates (**Fig. 3**). The hierarchical honeycombs are discretized using shell elements, while the remaining two plates are meshed with hexahedral elements. Of the two rigid plates, the top one has an initial velocity of 5 m/s, while the bottom one is fixed. The hierarchical honeycombs are made of aluminum alloy AA3030-H19, Young's modulus E = 69 GPa, Poisson's ratio v = 0.33, density ρ = 2700 kg/m^3, yield strength σ_{ys} = 115.8 MPa and ultimate tensile stress σ_{us} = 160 MPa [26]. The cell walls of the hierarchical honeycombs were modeled using the piecewise linear plasticity material model (MAT_24 in LS-DYNA) [27]. To simulate the contact between the two plates and the hierarchical honeycombs, two "automatic_nodes_to_surface" contacts with static and dynamic friction coefficients of 0.3 and 0.2 were used, respectively. Moreover, an "automatic_single_surface" contact was defined to simulate the contact within the hierarchical honeycomb itself during collapse [28].

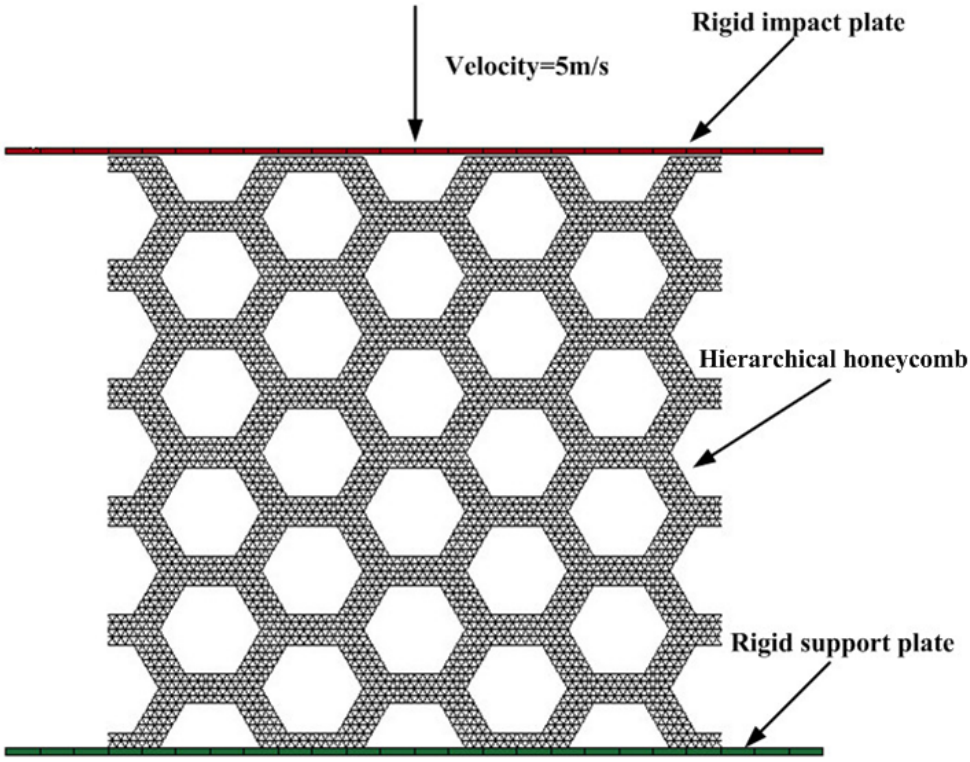

Fig. 3. FE model of the hierarchical honeycomb subject to in-plane loading.

2.3. Crashworthiness criteria

In this work, the mean crushing force (F_s) and the energy absorption (EA) are used as crashworthiness metrics. EA can be calculated as [31]:

$$EA(x) = \int_0^l F(x)dx \tag{5}$$

In Eq. (5), l indicates the total crushing distance (l = 60 mm in our cases). The variable x represents the crushing displacement, and F is the corresponding impact force. A higher value of EA indicates higher energy absorption capability. The mean crushing force F_s for a given deformation x can be expressed as:

$$F_S(x) = \frac{EA(x)}{x} \tag{6}$$

In general, the higher the mean crushing force F_s, the more efficient is the crashworthiness performance of a structure [32].

2.4. Validation of the FE modeling

To validate the computational framework used in this work, we have benchmarked our simulations with the ones related to a regular hexagonal honeycomb under in-plane dynamic loading with displacement control of 0.5 mm/min. [29]. **Figs. 4** and **5** show the comparison of our FE simulations with the experimental data. One can notice from **Fig. 4** that the numerically simulated deformations correlate well with those from the experiments. Moreover, the value of the crushing force obtained from the FE analysis is in excellent agreement with the one measured from the experiments (**Fig. 5**). The overall more than the satisfactory correlation between numerical and experimental results, in terms of both deformations and crushing force, show the baseline fidelity of the models developed here and their feasibility for being extended to the hierarchical honeycombs.

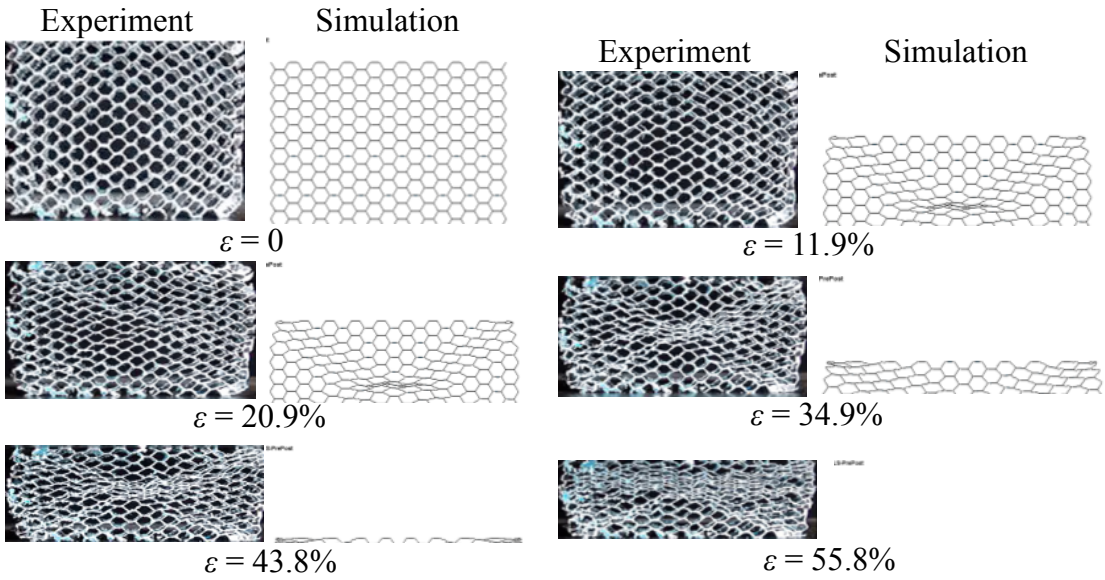

Fig. 4. Comparison of the deformations obtained from the finite element analysis and the experiment [28] related to a regular hexagonal honeycomb (Here ε denotes the nominal compressive strain).

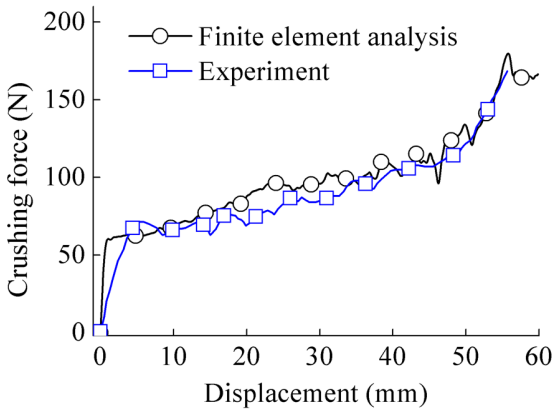

Fig. 5. Comparison of the crushing forces obtained from the finite element analysis and the experiment [28].

2.5. Sensitivity analysis of the mesh size

Previous studies have shown how the mesh size (i.e. the number of elements per cell wall thickness of the honeycomb) affects the accuracy of the finite element results [30]. This is particularly important for the case of hierarchical honeycombs and the converging values of the crushing force. We have therefore performed sensitivity analyses to determine the appropriate element size for the FE models. The simulated force-displacement curves for cell walls with 4 and 6 elements are compared in **Fig. 6**. It can be observed that the two

force-displacement curves are very similar, indicating that a minimum number of 4 elements per cell wall can provide a reasonable accuracy for our predictions.

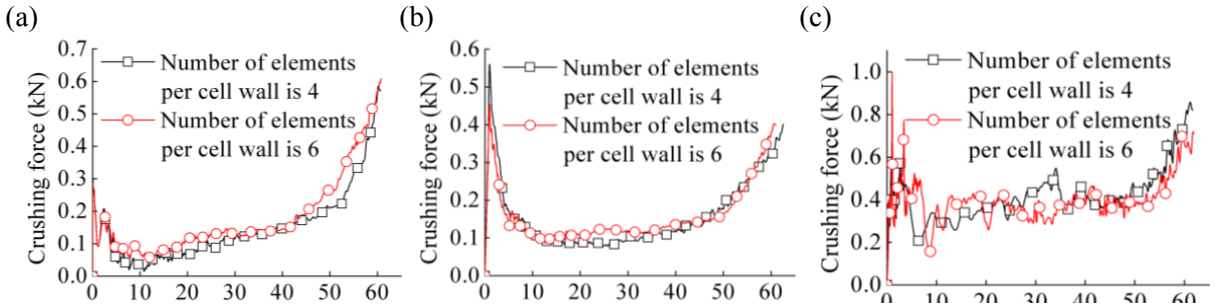

Fig. 6. Effect of the number of elements per cell wall on the crushing force of the hierarchical honeycombs. (a) Hexagonal, (b) Kagome, and (c) triangular

3. Numerical results and discussion

3.1. Comparison of different hierarchical honeycombs

Fig. 7 shows a direct comparison between the crushing forces of the three types of hierarchical honeycombs with the same r and N values. As a further benchmark, we have also considered the crushing force of the regular honeycomb (i.e., non-hierarchical) configuration. From observing **Fig.7**, one can distinctively notice that the crushing force of the triangular hierarchical honeycomb is the highest, and this is consistent with the fact that the triangular lattice configuration is the specific stiffest planar topology [33]. When N = 1, the crushing force of the regular honeycomb is higher than those of the Kagome and the hexagonal hierarchical honeycombs, however, it is lower than the one of the triangular hierarchical lattice. For N = 2 and 3, the crushing force of the regular honeycomb is generally higher than the one of the hexagonal hierarchical honeycomb, but lower than that the one shown by the Kagome hierarchical honeycomb.

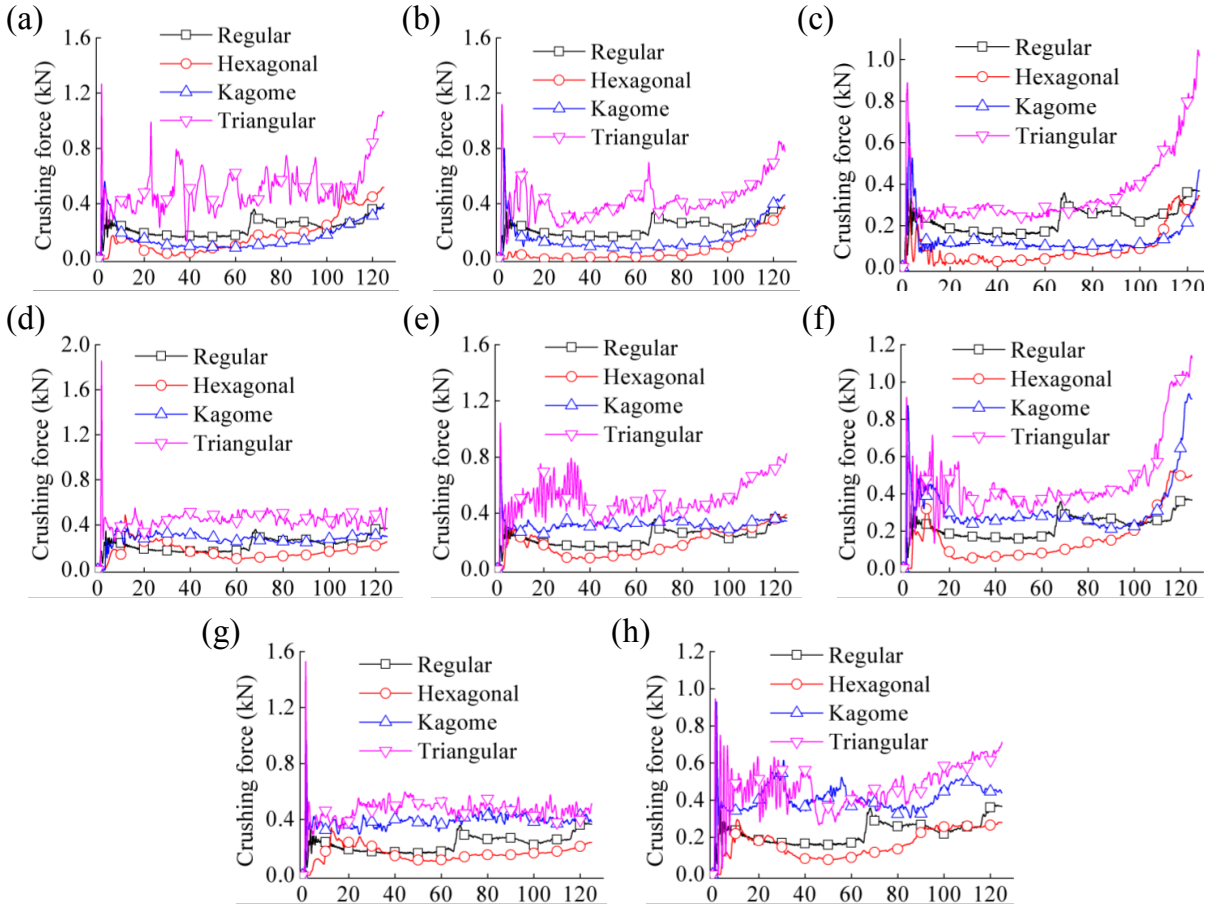

Fig. 7. Comparison of the crushing forces of the three hierarchical honeycombs with regular honeycomb. (a) $r = 1/5$, $N = 1$; (b) $r = 1/8$, $N = 1$; (c) $r = 1/11$, $N = 1$; (d) $r = 1/5$, $N = 2$; (e) $r = 1/8$, $N = 2$; (f) $r = 1/11$, $N = 2$; (g) $r = 1/8$, $N = 3$ and (h) $r = 1/11$, $N = 3$.

Fig. 8 shows the comparison of the *EAs* of the three hierarchical honeycombs with different geometric parameters N and r. It is worth reiterating that all the hierarchical honeycombs have the same weight, and in that sense, the results represent directly specific energy absorptions. The triangular hierarchical honeycomb features the best performance amongst the three hierarchical topologies, including the regular honeycomb case. The Kagome hierarchical configuration tends to have a lower specific energy (between 17% and 75% of the one shown by the triangular topologies). The lower performance is provided by the hexagonal hierarchical tessellations. The triangular hierarchical honeycomb with N=2 and r=1/8 features the best performance between the different tessellations, with over twice *EA* values than that of the regular honeycomb. Not all of the hierarchical honeycombs have, however, an improved performance compared to the hexagonal configuration: the hexagonal

hierarchical honeycomb has indeed a lower energy absorption capacity than the regular honeycomb. The Kagome hierarchical honeycomb with N = 2 and 3 has a better energy absorption than the regular honeycomb, however, the hierarchical version with N = 1 has a lower EA than the regular hexagonal configuration.

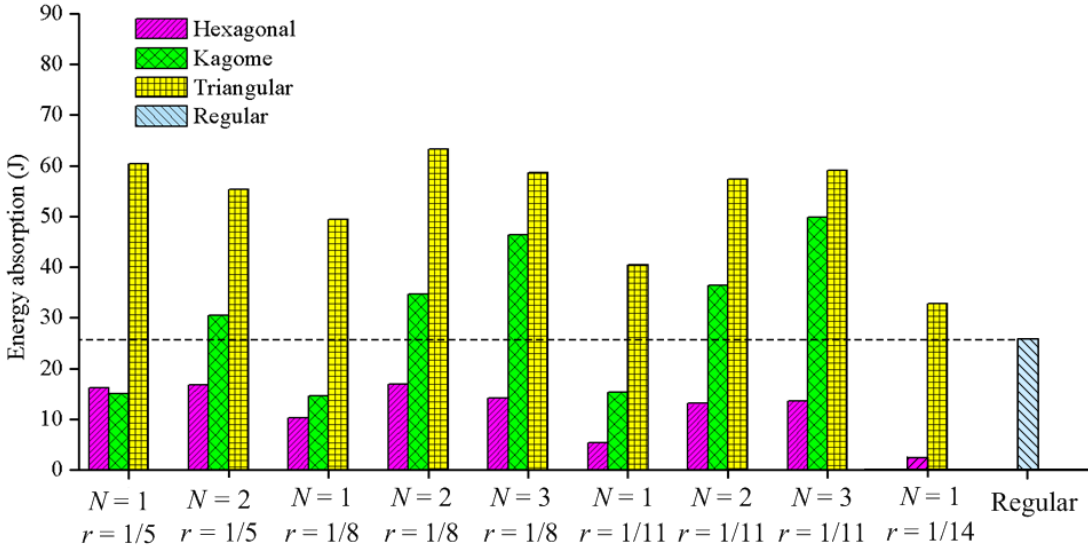

Fig. 8. Energy absorption of the hierarchical honeycombs with different geometric parameters.

3.2. Deformation modes

The average crushing force has a strict relation with the deformation mode of the structure [7], and therefore it is essential to understand the deformation mechanisms of the hierarchical honeycombs. **Figs. 9-11** shows the deformation modes of the three hierarchical honeycombs with r = 1/8 and N = 1 at different nominal compressive strains. The deformation modes of the three hierarchical honeycombs are quite evidently different from each other. Specifically, during the deformation of the hexagonal hierarchical honeycomb (**Fig. 9**), a V shape firstly occurs at the impact side due to the initiation of shear bands. The shear bands develop layer by layer until the hexagonal hierarchical honeycomb becomes compacted. The deformations of the Kagome hierarchical honeycomb are, however, different (**Fig. 10**). In this case, the shear band front initiates at the support side. With the increase of the impact displacement, the shear band appears at the impact side and then the center section collapses. The Kagome

hierarchical honeycomb is then crushed layer by layer until it is densified. The triangular hierarchical honeycomb is, however, subjected to an I-shaped band initially occurring at the indentation side (**Fig. 11**). A smaller shear band then appears at the support side, followed by a gradually collapse starting from the center. From the above observations, it is clear to infer that the filled substructures significantly affect the deformation modes of these hierarchical honeycombs.

To further understand the mechanical response of the proposed hierarchical honeycombs, local deformation patterns of the hierarchical honeycombs with $r = 1/8$ and $N = 1$ are shown in **Fig. 12**. One can see that the local deformation of the hexagonal hierarchical honeycomb was a "*Y*" shape cell. In the compressive process of the hexagonal hierarchical honeycomb, the "*Y*" shape cell would rotate around the cross center until it was compacted. While the representative deformable cells for the Kagome and triangular hierarchical honeycombs were an "*X*" shape cell and a "six-side-cross" shape cell, respectively. Similarly, when the Kagome and triangular hierarchical honeycombs were crushed, the "*X*" and "six-side-cross" shape cells would rotate around their cross centers, respectively, until they were compacted. Generally, the rotation of the "six-side-cross" shape cell could absorb more dynamic energy than the rotations of the "*Y*" and "*X*" shape cells. This is the reason why the triangular hierarchical honeycomb exhibits a better energy absorption capacity than the other two hierarchical honeycombs.

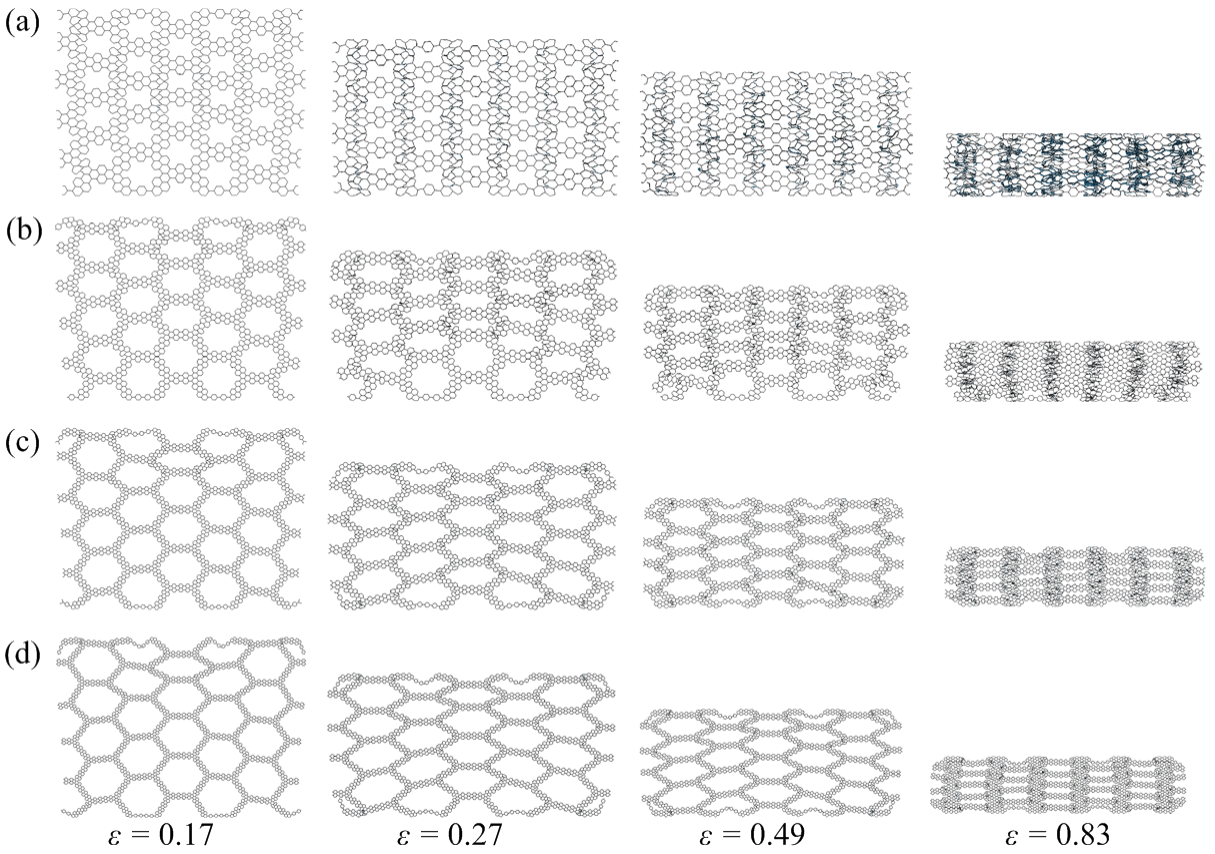

Fig. 9. FE predicted deformation modes of the hexagonal hierarchical honeycombs with r = 1/8 and N = 1 under different nominal compressive strains.

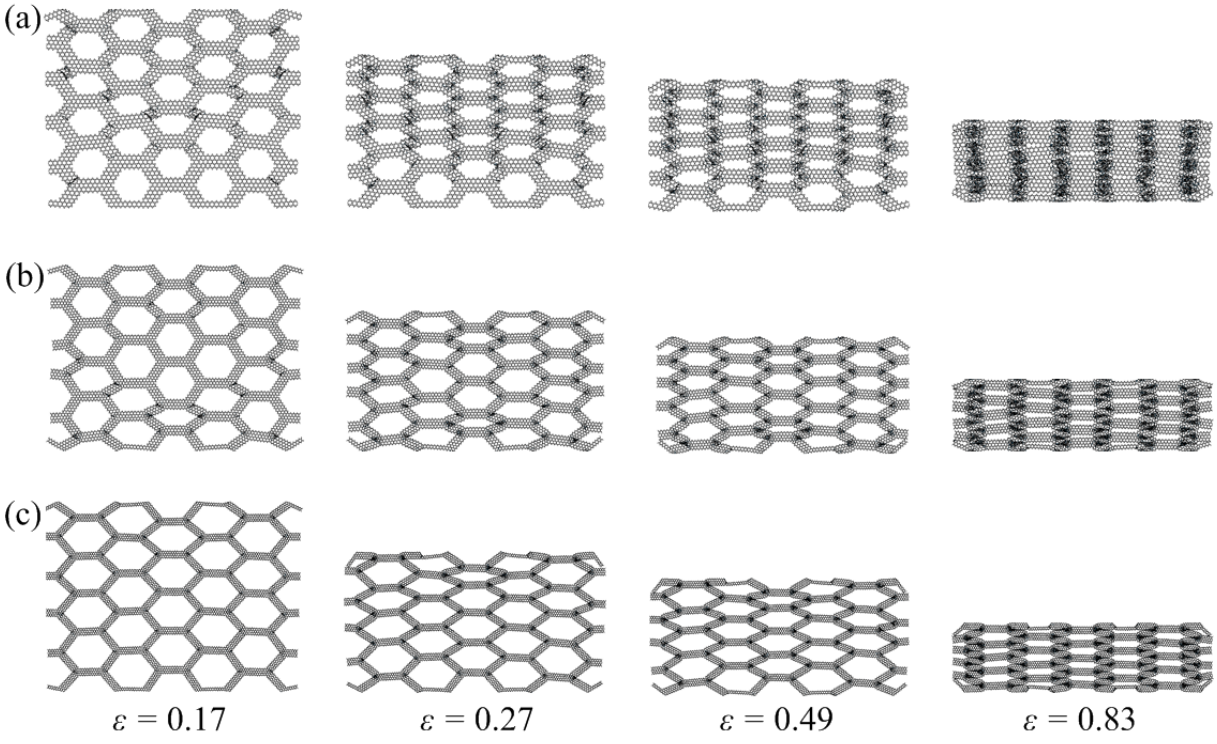

Fig. 10. FE predicted deformation modes of the Kagome hierarchical honeycombs with r =

1/8 and $N = 1$ under different nominal compressive strains.

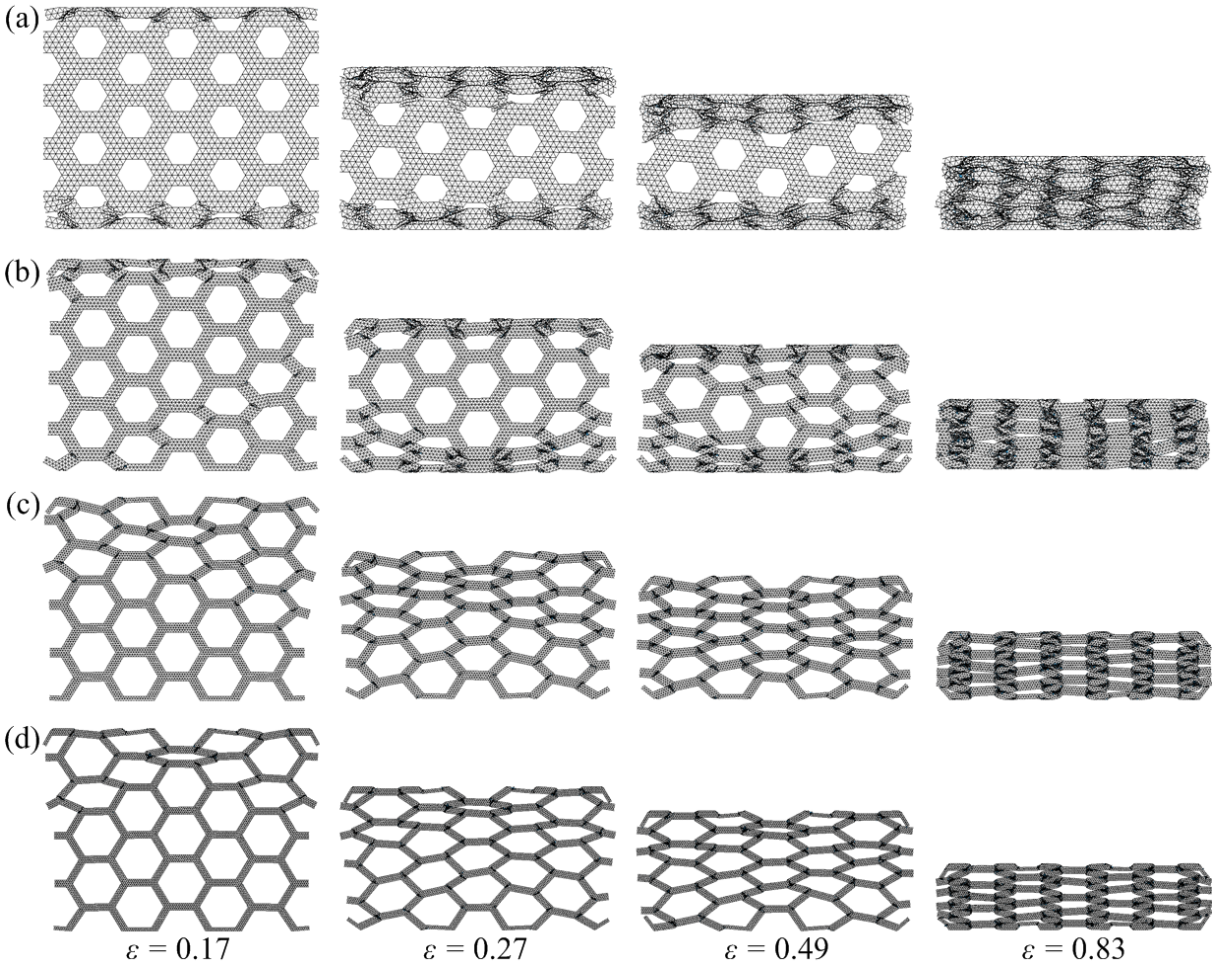

Fig. 11. FE predicted deformation modes of the triangular hexagonal hierarchical honeycombs with $r = 1/8$ and $N = 1$ under different nominal compressive strains.

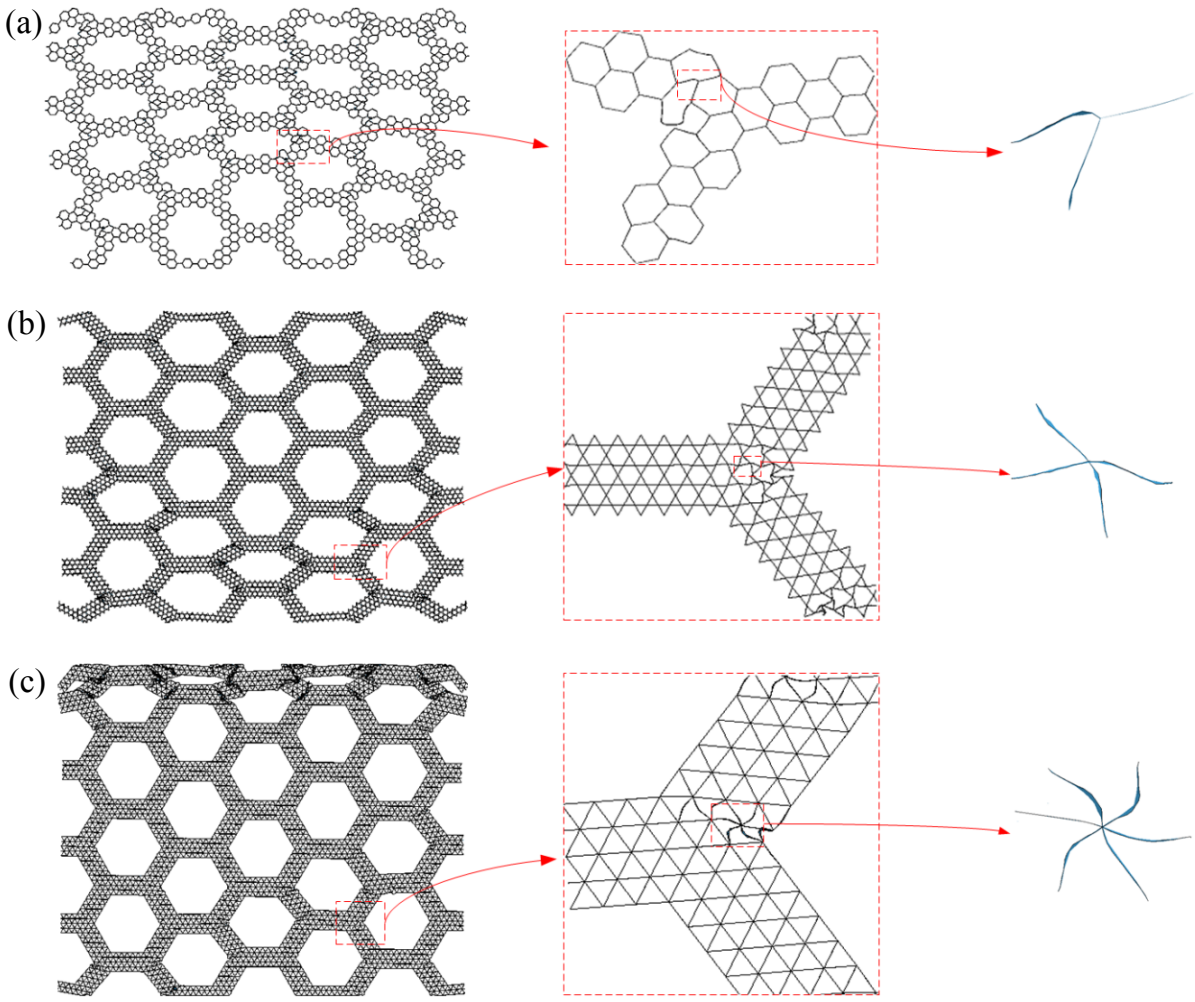

Fig. 12. Local deformation patterns of the hierarchical honeycombs with $r = 1/8$ and $N = 1$. (a) Hexagonal, (b) Kagome and (c) triangular.

3.3. Hexagonal hierarchical honeycombs

Figs. 13 and **14** show the force-displacement relations of the hierarchical honeycombs with different N and r. The mean crushing forces are calculated using Eq. (6) and are summarized in **Fig. 15**. The function $F(x)$ in Eq. (6) is the transient crushing force. From **Fig. 15**, one can notice that the mean crushing force of the hexagonal hierarchical honeycomb is sensitive to the design variables N and r. The average crushing force increases with the increase of N (**Fig. 15** (a)), while it decreases for increasing r values (**Fig. 15** (b)). The hexagonal hierarchical honeycomb with $N = 2$ and $r = 1/5$ has the highest mean crushing force among all the considered cases. The hexagonal hierarchical honeycomb with $N = 1$ and $r = 1/14$ has, however, the worst mean crushing force value within the hierarchical cellular structures considered here. These geometric analyses indicate that the N and r parameters significantly

affect the crushing forces of the hexagonal hierarchical honeycombs.

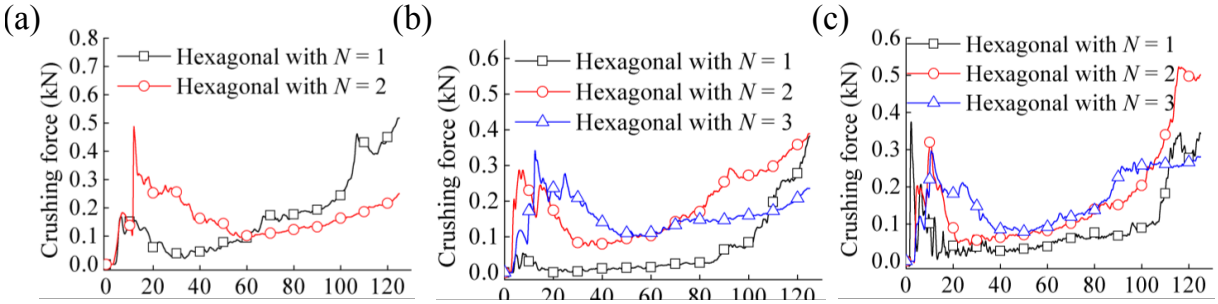

Fig. 13. Comparison of mean crushing forces of hexagonal hierarchical honeycomb with different N. (a) r = 1/5; (b) r = 1/8 and (c) r = 1/11.

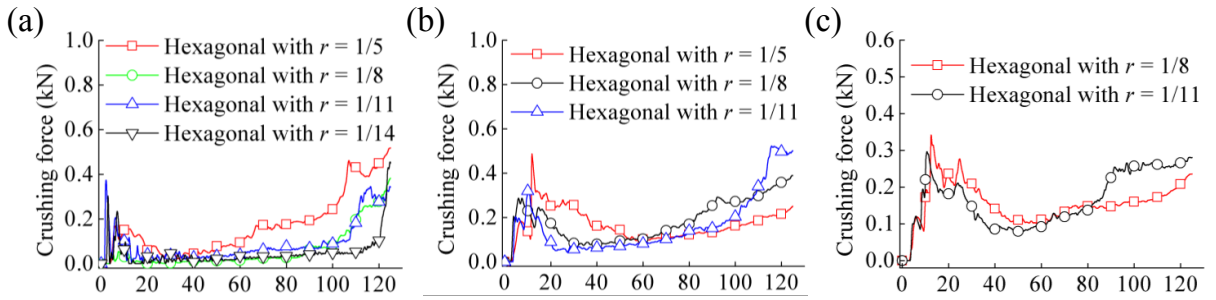

Fig. 14. Comparison of crushing forces of the hexagonal hierarchical honeycombs with different r. (a) N = 1; (b) N = 2 and (c) N = 3.

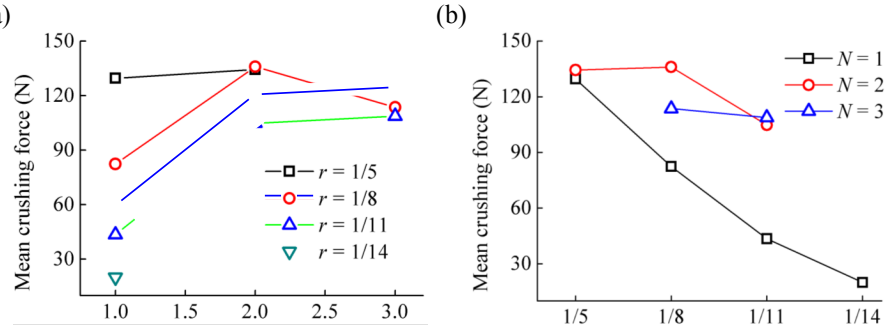

Fig. 15. Effect of geometric parameters on the mean crushing force of the hexagonal hierarchical honeycomb. (a) N and (b) r.

3.4. Kagome hierarchical honeycombs

Fig. 18 shows the variation of the mean crushing force of the Kagome hierarchical honeycomb when the N and r parameters change, which were calculated from the force-displacement curves, as shown in **Figs 16** and **17**. The crushing force of the Kagome

configuration with larger N values is higher than the one related to the topology with smaller N (**Fig. 16**). From **Fig. 17**, one can also observe that the crushing force-displacement curves of the Kagome lattices with different values of r have almost the same values. We note that the mean crushing forces of these honeycombs are quite sensitive to the variable N, but less so when it concerns the r parameter (**Fig. 18**). When the value of N increases, the mean crushing force tends to become larger. When the parameter r increases, however, the change of the average crushing force is limited. In particular, the Kagome hierarchical honeycomb with N = 3 and r = 1/11 shows the highest mean crushing force, while the structure with N = 1 and r = 1/8 has the lowest one. These results are quite different from the ones related to the hexagonal hierarchical honeycomb configuration.

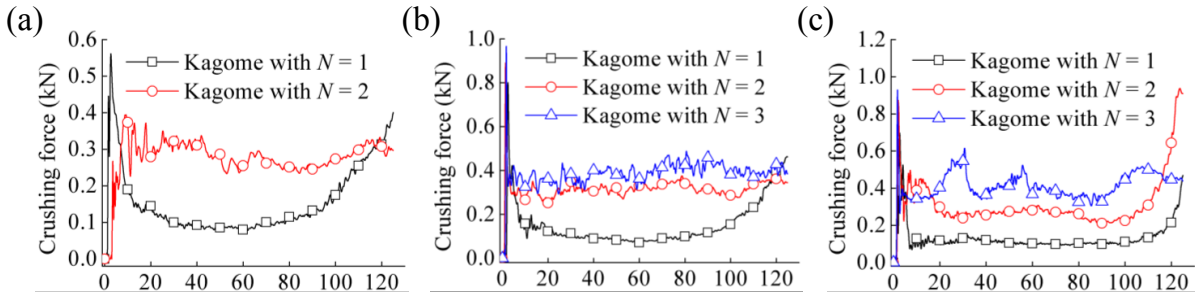

Fig. 16. Comparison of crushing forces of the Kagome hierarchical honeycombs with different N: (a) r = 1/5; (b) r = 1/8 and (c) r = 1/11.

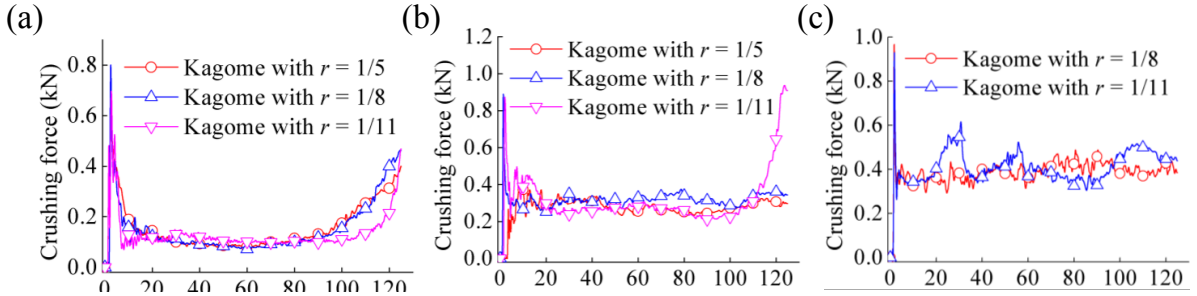

Fig. 17. Comparison of crushing forces of the Kagome hierarchical honeycombs with different r. (a) N = 1; (b) N = 2 and (c) N = 3.

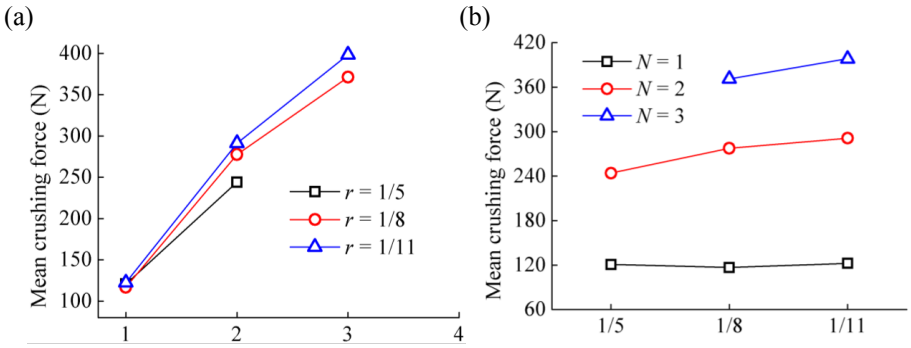

Fig. 18. Effect of geometric parameters on the mean crushing force of the Kagome hierarchical honeycomb. (a) *N* and (b) *r*.

3.5. Triangular hierarchical honeycombs

Figs. 19 and **20** show the force-displacement curves related to the triangular hierarchical honeycombs, all displaying a noticeable plateau region that indicates the presence of a stable collapse deformation. Before the compaction of the triangular honeycombs, the crushing forces oscillate between 200 N and 600 N. This is an indication that the triangular hierarchical honeycomb could feature a high crushing force efficiency [29] for impact engineering applications. **Fig. 21** shows the effect of the variables *N* and *r* on the mean crushing force of the triangular hierarchical honeycomb, which was calculated from the force-displacement curves shown in **Figs 19** and **20**. The *N* and *r* parameters both affect the mean crushing force significantly, which does not monotonically increase or decrease for increasing *N* values. For the *r* = 1/5 case, the mean crushing force decreases for higher values of *N*. For the case of *r* = 1/8, however, the mean crushing force increases with the increase of *N* from 1 to 2, and then decreases for *N* passing from 2 to 3. In the case of *r* = 1/11, the mean crushing force tends to monotonically increase higher *N*. On the opposite, when *r* increases, the variation of the mean crushing force is more complex. For the triangular lattice at *N* = 1, the mean crushing force monotonously decreases with increasing *r* values. For the case *N* = 2 instead, the mean crushing force first increases for values of between *r* = 1/5 and *r* = 1/8 and then decreases from *r* = 1/8 to *r* = 1/11. In the case of the triangular hierarchical honeycomb with *N* = 3, one can observe only a slight variation of the mean crushing force with the increase of *r*. By observing **Fig. 21**, one can notice that the triangular hierarchical honeycomb with *N* = 2 and *r* = 1/8 features the highest mean crushing force, and therefore the best energy absorption

capacity amongst the lattices considered in this work.

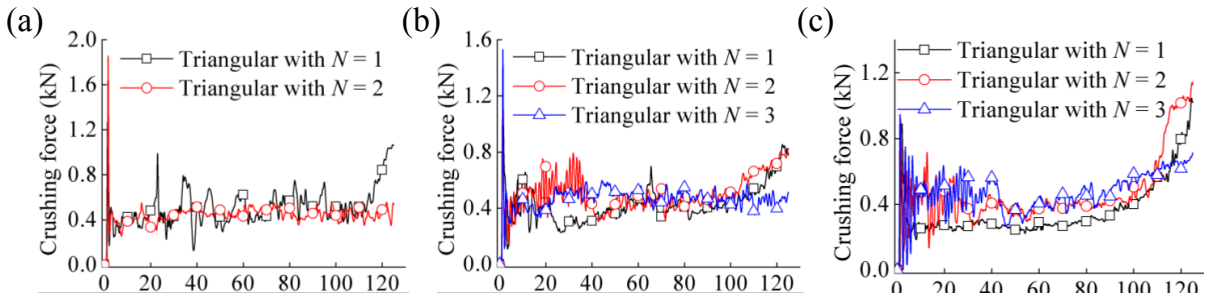

Fig. 19. Comparison of crushing forces of the triangular hierarchical honeycombs with different N. (a) r = 1/5; (b) r = 1/8 and (c) r = 1/11.

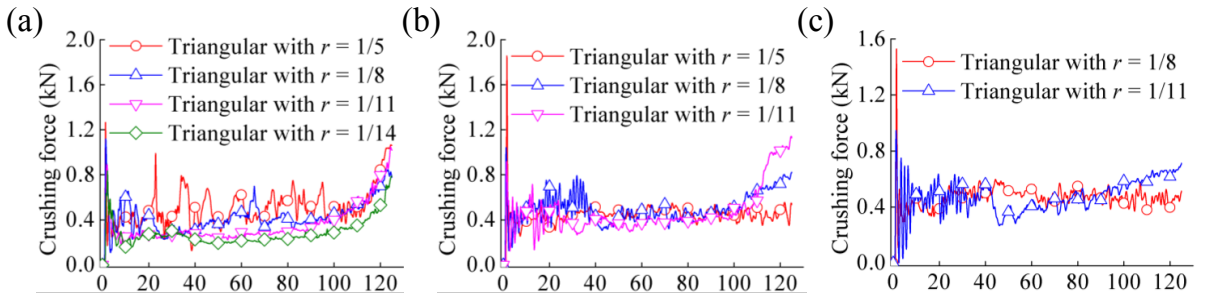

Fig. 20. Comparison of crushing forces of the triangular hierarchical honeycombs with different r. (a) N = 1; (b) N = 2 and (c) N = 3.

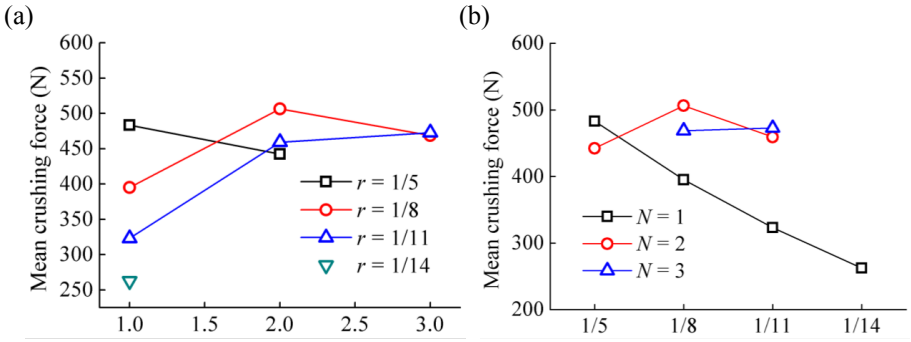

Fig. 21. Effect of geometric parameters on the mean crushing force of the triangular hierarchical honeycomb. (a) N and (b) r.

4. Conclusions

In this work, we have investigated, by using the nonlinear finite element code LS-DYNA, the

energy absorption property of three types of hierarchical honeycombs with different configurations under in-plane dynamic loading. As a further benchmark, we have also considered a reference and non-hierarchical hexagonal honeycomb configuration. Our numerical simulations indicate that triangular hierarchical lattice features the best energy absorption capacity. The triangular hierarchical topology also performs significantly better than the regular honeycomb in terms of crashworthiness. In particular, the triangular hierarchical honeycomb with geometry design variables equal to $N = 2$ and $r = 1/8$ has the highest crushing resistance performance, with over twice the value of absorbed energy compared to the regular honeycomb. In this regard, triangular hierarchical honeycomb can be considered to replace the regular honeycomb configuration in the field of the impact engineering for safety protection. We also observe that for the hexagonal and Kagome hierarchical honeycombs with parameters equal to $N = 1$ and $r = 1/8$, the collapse modes follow a shear band "*V*" shape. While for the triangular hierarchical honeycomb with $N = 1$ and $r = 1/8$, the collapse mode is, however, composed of a mix of compressive "*I*" and the shear band "*V*" shapes. Further parametric analyses suggest that the energy absorptions of the hexagonal and triangular hierarchical honeycombs are quite sensitive to the design variables N and r. For the Kagome hierarchical honeycomb, the effect of the parameter N on its energy absorption is significant, however, the influence of the design variable r is almost negligible. The numerical simulations presented here not only provide us a better understanding on the dynamic response of a new type of cellular structures, but also offer new opportunities for the design of structured materials capable of achieving extreme and customizable energy absorption properties that can be of particular interest for applications in automotive, aerospace, semiconductor, and energy. Future work will be redirected toward the advanced fabrication and high strain rate mechanical testing of the proposed hierarchical honeycombs with different materials and length scales.

Acknowledgements

Dr. H. Yin, X. Huang, and Dr. G. Wen thank the financial support from the State Key Laboratory of Advanced Design and Manufacturing for Vehicle Body (No. 51775001), the Young Teacher Development Plan of Hunan University of China, and the support from the

Collaborative Innovation Center of Intelligent New Energy Vehicle and the Hunan Collaborative Innovation Center of Green Automobile.

References

[1] Zhang QC, Yang XH, Li P, Huang GY, Feng SS, Shen C, Han B, Zhang XH, Jin F, Xu F, Lu TJ. Bioinspired engineering of honeycomb structure - using nature to inspire human innovation, Progress in Materials Science 2015; 74: 332–400.

[2] Lu GX, Yu TX. Energy absorption of structures and materials. Boca Raton: CRC Press; 2003.

[3] Gibson LJ, Ashby MF. Cellular solids: structure and properties. 2nd ed. Cambridge; Cambridge University Press; 1997.

[4] Wierzbicki T. Crushing analysis of metal honeycombs. International Journal of Impact Engineering 1983; 1(2): 157–174.

[5] Wu EB, Jiang WS. Axial crush of metallic honeycombs. International Journal of Impact Engineering 1997; 19(5-6): 439–456.

[6] Cricrì G, Perrella M, Calì C. Honeycomb failure processes under in-plane loading. Composites: Part B 2013; 45: 1079–1090.

[7] Papka SD, Kyriakides S. Experiments and full-scale numerical simulations of in-plane crushing of a honeycomb. Acta Materialia 1998; 46(8): 2765–2776.

[8] Ruan D, Lu GX, Wang B, Yu TX. In-plane dynamic crushing of honeycombs—a finite element study. International Journal of Impact Engineering 2003; 28(2): 161–182.

[9] Lakes R. Materials with structural hierarchy. Nature 1993; 361: 511–515.

[10] Peter F, Richard W. Nature's hierarchical materials. Progress in Materials Science 2007; 52(8): 1263–1334.

[11] Chen, Y., and Wang. Harnessing structural hierarchy to design stiff and lightweight phononic crystals. Extreme Mechanics Letters 2016; 9: 91-96.

[12] Zheng XY, Smith W, Jackson J, Moran B, Cui HC, Chen D, Ye JC, Fang N, Rodriguez N, Weisgraber T, Spadaccini CM. Multiscale metallic metamaterials. Nature Materials 2016; 15: 1100–1106.

[13] Vigliotti A, Pasini D. Mechanical properties of hierarchical lattices. Mechanics of

Materials 2013; 62(15): 32–43.

[14] Sun FF, Lai CL, Fan HL, Fang DN. Crushing mechanism of hierarchical lattice structure. Mechanics of Materials 2016; 97: 164–183.

[15] Zheng JJ, Zhao L, Fan HL. Energy absorption mechanisms of hierarchical woven lattice composites. Composites: Part B 2012; 43: 1516–1522.

[16] Zhang Y, Lu MH, Wang CH, Sun GY, Li GY. Out-of-plane crashworthiness of bio-inspired self-similar regular hierarchical honeycombs. Composite Structures 2016; 144: 1–13.

[17] Sun GY, Jiang H, Fang JG, Li GY, Li Q. Crashworthiness of vertex based hierarchical honeycombs in out-of-plane impact. Materials & Design 2016; 110: 705–719.

[18] Zhao L, Zheng Q, Fan HL, Jin FN. Hierarchical composite honeycombs. Materials & Design 2012; 40: 124–129.

[19] Sun YT, Pugno N. In plane stiffness of multifunctional hierarchical honeycombs with negative Poisson's ratio sub-structures. Composite Structures 2013; 106: 681–689.

[20] Sun YT, Wang B, Pugno N, Wang B, Ding Q. In-plane stiffness of the anisotropic multifunctional hierarchical honeycombs. Composite Structures 2015; 131: 616–624.

[21] Chen Q, Pugno N. In-plane elastic buckling of hierarchical honeycomb materials. European Journal of Mechanics - A/Solids 2012; 34: 120-129.

[22] Chen Q, Pugno N. In-plane elastic properties of hierarchical nano-honeycombs: the role of the surface effect. European Journal of Mechanics - A/Solids 2013; 37: 248-255.

[23] Qiao JX, Chen CQ. In-plane crushing of a hierarchical honeycomb. International Journal of Solids and Structures 2016; 85-86: 57–66.

[24] Chen, Y., Li, T., Jia, Z., Scarpa, F., Yao, C. W., and Wang, L. 3D printed hierarchical honeycombs with shape integrity under large compressive deformations. Materials & Design 2017; 137:226-234.

[25] Chen YY, Jia Z, Wang LF. Hierarchical honeycomb lattice metamaterials with improved thermal resistance and mechanical properties. Composite Structures 2016; 152: 395–402.

[26] Sun GY, Li SF, Liu Q, Li GY, Li Q. Experimental study on crashworthiness of empty/aluminum foam/honeycomb-filled CFRP tubes. Composite Structures 2016; 152: 969–993.

[27] LSTC. LS-DYNA keyword user's manual, version 971. Livermore (CA): Livermore Software Technology Corporation; 2007.

[28] Yin HF, Xiao YY, Wen GL, Qing QX, Wu X. Crushing analysis and multi-objective optimization design for bionic thin-walled structure. Materials & Design 2015; 87: 825–834.

[29] Khan MK, Baig T, Mirza S. Experimental investigation of in-plane and out-of- plane crushing of aluminum honeycomb. Materials Science and Engineering A 2012; 539: 135–142.

[30] Feng H, Cui XY, Li GY. A stable nodal integration method with strain gradient for static and dynamic analysis of solid mechanics. Engineering Analysis with Boundary Elements 2016; 62: 78–92.

[31] Tang T, Zhang WG, Yin HF, Wang H. Crushing analysis of thin-walled beams with various section geometries under lateral impact. Thin-Walled Structures 2016; 102: 43–57.

[32] Zhang X, Zhang H. Axial crushing of circular multi-cell columns. International Journal of Impact Engineering 2014; 65: 110–125.

[33] Gibson, L. J., and Ashby, M. F. Cellular solids: structure and properties. 1999; Cambridge University Press.